

Supporting Information

A Flexible Rechargeable Zinc-Ion Wire-shaped Battery with Shape Memory Function

Zifeng Wang,^a Zhaoheng Ruan,^a Zhuoxin Liu,^a Yukun Wang,^a Zijie Tang,^a Hongfei Li,^a

Minshen Zhu,^a Tak Fuk Hung,^a Jun Liu,^b Zicong Shi,^b and Chunyi Zhi^{a*}

a. Department of Materials Science and Engineering, City University of Hong Kong, 83 Tat

Chee Avenue, Kowloon, Hong Kong Special Administrative Region, China

b. School of Material and Energy, Guangdong University of Technology, Guangzhou,

510006, PR China

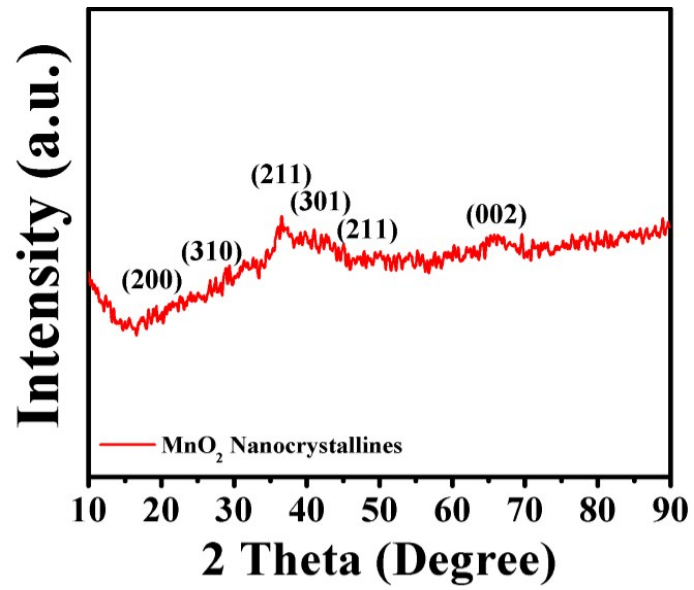


Figure S1. X-ray diffraction pattern of the electrodeposited MnO₂ nanocrystallines (PDF#44-0141).

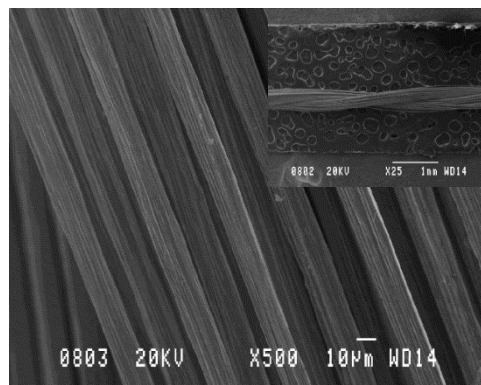


Figure S2. Typical SEM image of pristine stainless steel yarn. Inset figure shows the twisting shape of the yarn.

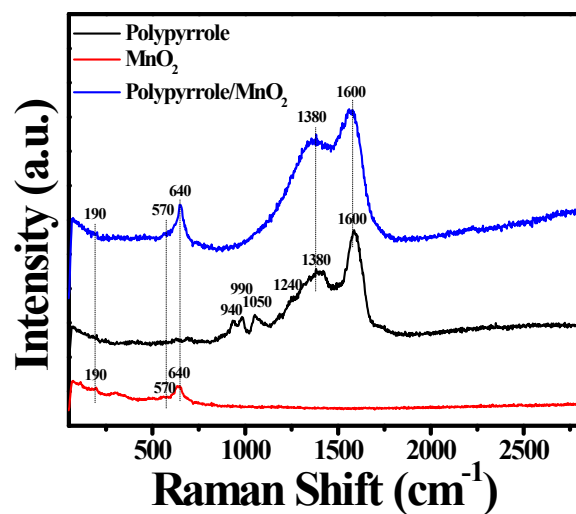


Figure S3. Raman spectra of electrodeposited Polypyrrole, MnO_2 and Polypyrrole coated MnO_2 .

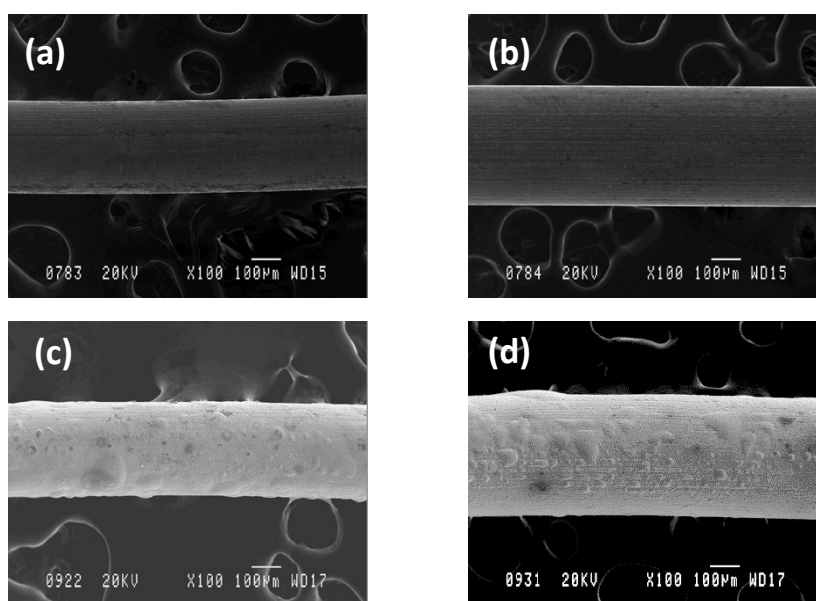


Figure S4. SEM images of pristine nitinol wires and Zn electrodeposited nitinol wires of different diameters. (a) and (b) SEM images of 0.012 inch and 0.016 inch nitinol wires, respectively; (c) and (d) Zn electrodeposited nitinol wires with diameters of 0.012 and 0.016 inch, respectively.

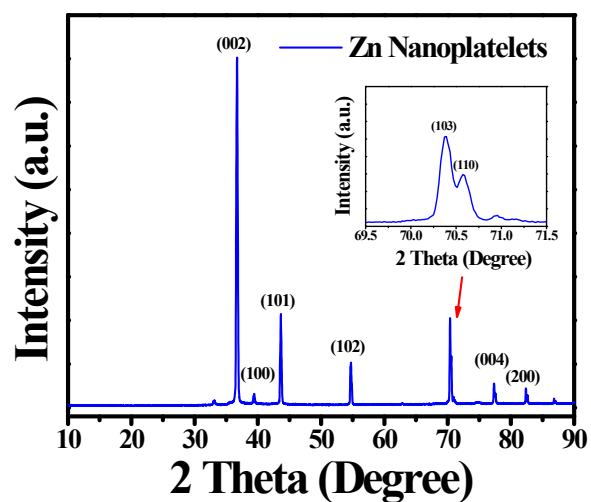


Figure S5. X-ray diffraction pattern of the electrodeposited Zn nanoplatelets (PDF#87-0713);

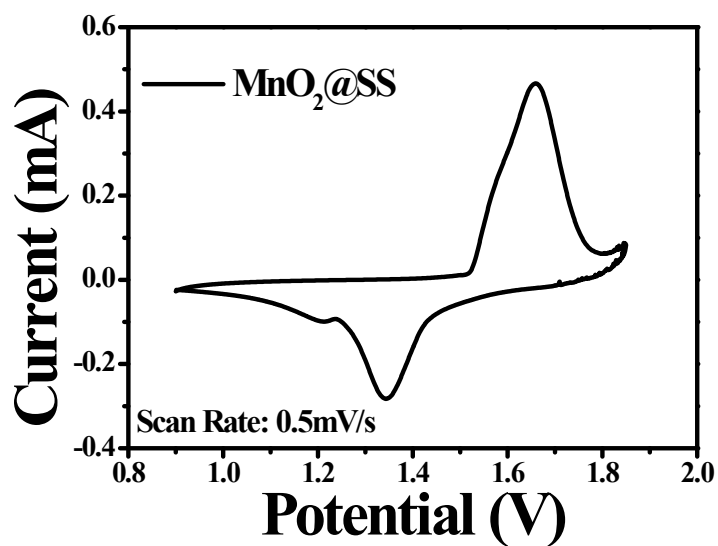


Figure S6. Cyclic voltammetry study of electrodeposited MnO₂ on stainless steel at 0.5mV/s scan rate.

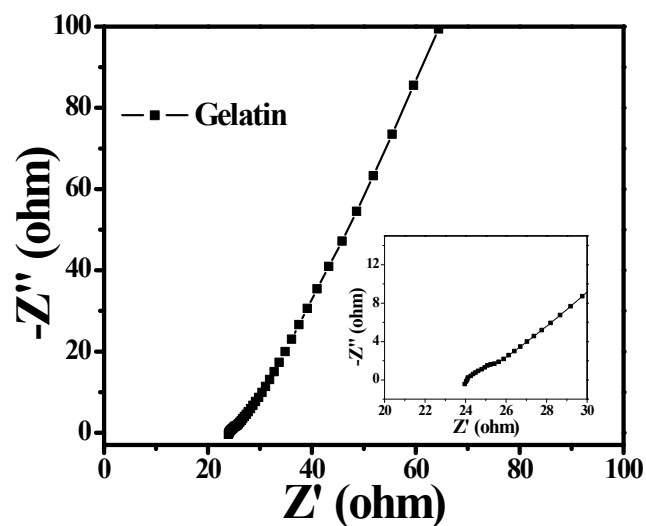


Figure S7. Electrochemical impedance study of gelatin electrolyte without the addition of borax.

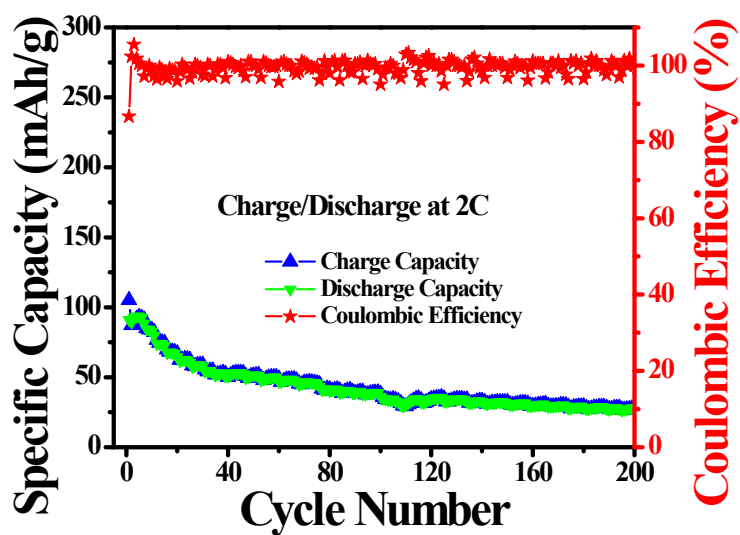


Figure S8. Cyclic stability of Zn@NT-MnO₂@SS without PPy coating at 2 C current density.

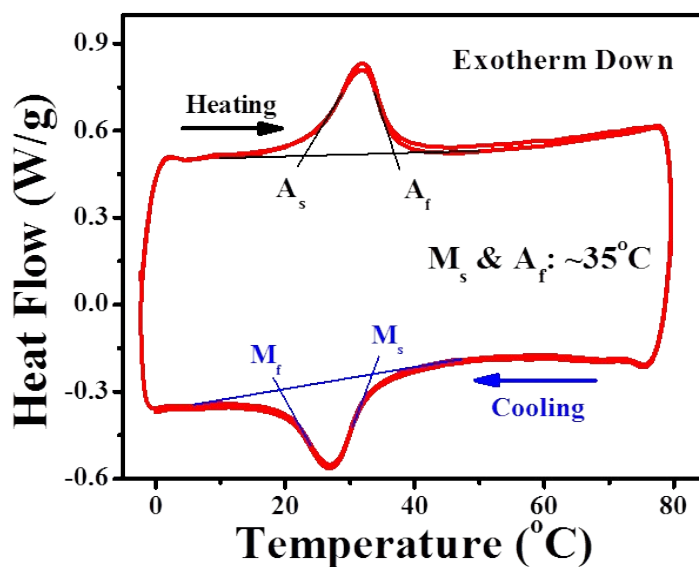


Figure S9. Differential scanning calorimetry study of pristine nitinol wire, showing the phase transition temperatures of the NiTi phase. The four markers, which are A_s , A_f , M_f and M_s on the curve represent the corresponding phase transition temperature determined by DSC analysis, in which A_s and A_f represent the starting and finishing temperatures of the austenitic transition whereas the M_s and M_f represent the corresponding temperatures of martensitic transition of the NiTi alloy.

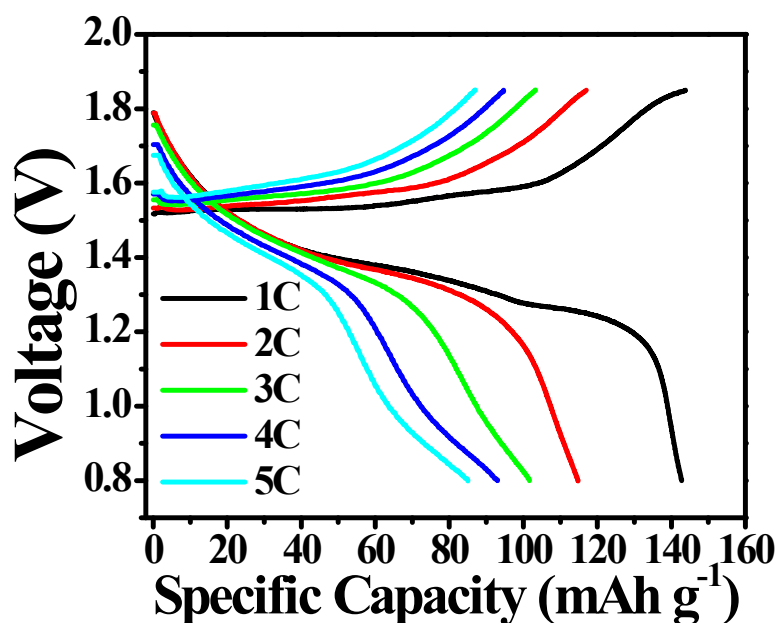


Figure S10. The charge/discharge curves of the Zn@NT-MnO₂/PPy@SS battery in aqueous electrolyte at 1 to 5 C current densities, respectively.

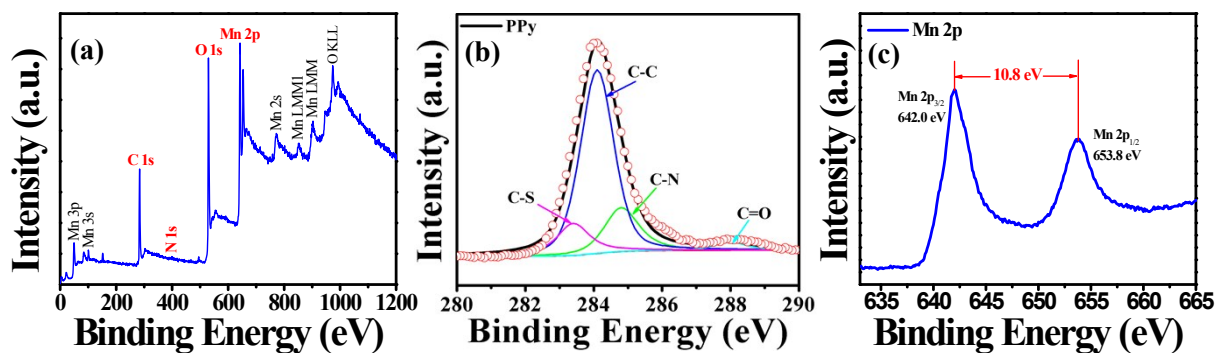


Figure S11. XPS spectra of MnO₂ coated with PPy. (a) XPS survey spectra reviewing the component elements of MnO₂ coated with PPy; (b) High resolution C 1s spectrum showing the characteristics of PPy and the corresponding bonds; (c) High resolution Mn 2p spectrum showing the characteristics of MnO₂.

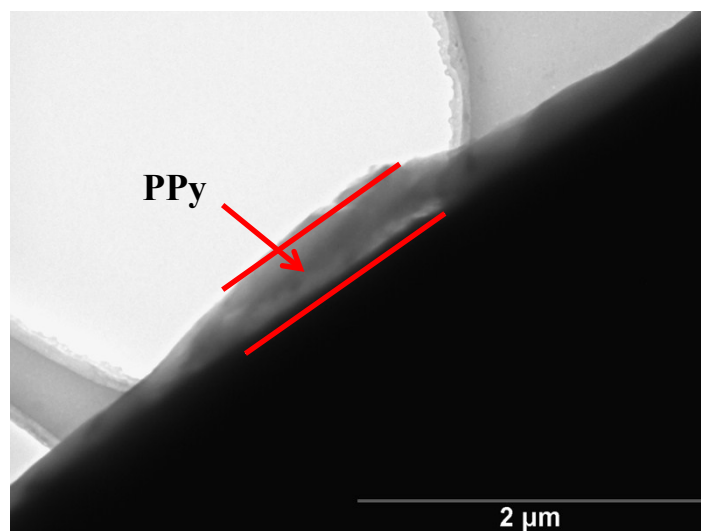


Figure S12. Typical TEM image of the MnO₂ electrode material coated with PPy, the different morphology indicates the existence of the electrodeposited PPy film.

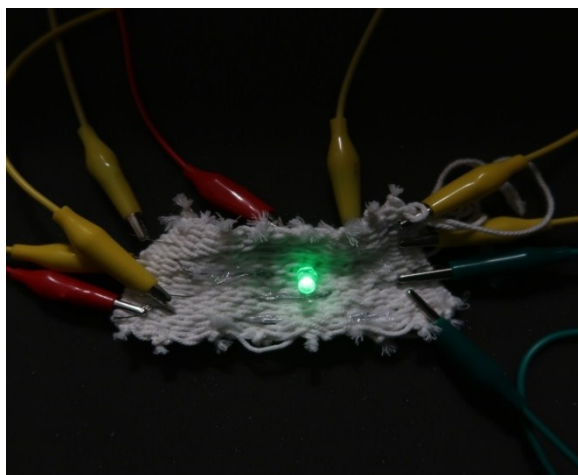


Figure S13. Picture showing the textile woven by cotton yarn and the SMWB and successfully powering of a green light LED bulb.